Temperature-Programmed Desorption (TPD) and Density Functional Theory (DFT) Study

Comparing the Adsorption of Ethyl Halides on the Si(100) Surface

Jing Zhao[1], Benjamin W. Noffke[2], Krishnan Raghavachari[2], and Andrew V. Teplyakov[1]*

[1]Department of Chemistry and Biochemistry, University of Delaware, Newark, DE 19716

[2]Department of Chemistry, Indiana University, Bloomington, IN 47405

Supporting Information

Computational Details

The Gaussian09 program suite was used to calculate energies and zero-point energy corrections. The B3LYP, M06, and M06-2X density functionals were used with and without Grimme's D3 empirical dispersion corrections. Optimization and frequency calculations were performed with the 6-311+G(3df,p) basis set, which for iodine atoms, is an in-house custom basis set with the coefficients listed below. For accurate single point energies, the aug-cc-pVTZ basis set was used for hydrogen, carbon, silicon, and chlorine atoms and the aug-cc-pVTZ-PP basis set was used for iodine atoms. An ultrafine grid was used for all calculations. The zero-point energies from the frequency calculation are added to these single point energies and the zero-point corrected energies are used to construct energy profiles to describe the dissociation of ethylhalides on a Si(100) dimer cluster Si_9H_{12}. For these energy profiles, all stages of the reaction are relative to the energy of EtX + Si(100) at infinite separation. Transition state guesses were obtained by performing relaxed internal coordinate scans for the ethylhalide bond dissociation. The transition state structure guess is then optimized and verified to have one imaginary frequency.

Complete Reference 23:

Gaussian 09, Revision **D.01**, Frisch, M. J.; Trucks, G. W.; Schlegel, H. B.; Scuseria, G. E.; Robb, M. A.; Cheeseman, J. R.; Scalmani, G.; Barone, V.; Mennucci, B.; Petersson, G. A.; Nakatsuji, H.; Caricato, M.; Li, X.; Hratchian, H. P.; Izmaylov, A. F.; Bloino, J.; Zheng, G.; Sonnenberg, J. L.; Hada, M.; Ehara, M.; Toyota, K.; Fukuda, R.; Hasegawa, J.; Ishida, M.; Nakajima, T.; Honda, Y.; Kitao, O.; Nakai, H.; Vreven, T.; Montgomery, J. A., Jr.; Peralta, J. E.; Ogliaro, F.; Bearpark, M.; Heyd, J. J.; Brothers, E.; Kudin, K. N.; Staroverov, V. N.; Kobayashi, R.; Normand, J.; Raghavachari, K.; Rendell, A.; Burant, J. C.; Iyengar, S. S.; Tomasi, J.; Cossi, M.; Rega, N.; Millam, N. J.; Klene, M.; Knox, J. E.; Cross, J. B.; Bakken, V.; Adamo, C.; Jaramillo, J.; Gomperts, R.; Stratmann, R. E.; Yazyev, O.; Austin, A. J.; Cammi, R.; Pomelli, C.; Ochterski, J. W.; Martin, R. L.; Morokuma, K.; Zakrzewski, V. G.; Voth, G. A.; Salvador, P.; Dannenberg, J. J.; Dapprich, S.; Daniels, A. D.; Farkas, Ö.; Foresman, J. B.; Ortiz, J. V.; Cioslowski, J.; Fox, D. J. Gaussian, Inc., Wallingford CT, 2009.

Evaluating Basis Set Superposition Errors

We have included the results for the counterpoise corrections for the interaction complexes for EtI and EtCl. To examine the basis set effect, we have used the M06-D3 functional with the cc-pVDZ, aug-cc-pVDZ, cc-pVTZ, aug-cc-pVTZ, and 6-311+G(3df,p) basis sets to evaluate these corrections (Table S1). The counterpoise corrections for EtI are not consistently larger than that for EtCl, especially for the correlation consistent basis sets. The correlation consistent triple-zeta basis sets show a very small error, with little difference when diffuse functions are added.

Table S1. This table shows the basis set superposition errors for the M06-D3 functional and the cc-pVDZ, aug-cc-pVDZ, cc-pVTZ, aug-cc-pVTZ, and 6-311+G(3df,p) basis sets.

Basis Set Superposition Errors (kJ/mol)		
Basis Set	EtCl	EtI
cc-pVDZ	7.31	5.41
aug-cc-pVDZ	5.53	5.82
cc-pVTZ	3.46	2.74
aug-cc-pVTZ	3.31	2.97
6-311+G(3df,p)	5.12	6.91

The other functionals, B3LYP and M06-2X, have their counterpoise corrections calculated for the aug-cc-pVTZ basis set. Table S2 summarizes the basis set superposition errors for all of the functionals with dispersion and Table S3 summarizes the errors without dispersion. M06 and M06-2X show no difference with respect to dispersion corrections, which is expected because of their inherent parameterization of dispersion. B3LYP results with and without dispersion vary slightly and the counterpoise correction is about 1.5 kJ/mol. All of the functionals have a low counterpoise correction for the aug-cc-pVTZ basis set..

Table S2. Summary of the basis superposition errors for the M06-D3, B3LYP-D3, and M06-2X-D3 functionals with the aug-cc-pVTZ basis set. All energies are given in kJ/mol.

Basis Set Superposition Errors (kJ/mol)					
M06-D3		B3LYP-D3		M06-2X-D3	
EtCl	EtI	EtCl	EtI	EtCl	EtI
3.31	2.97	1.53	1.55	2.13	1.72

Table S3. Summary of the basis superposition errors for the M06, B3LYP, and M06-2X functionals with the aug-cc-pVTZ basis set. All energies are given in kJ/mol.

| Basis Set Superposition Errors (kJ/mol)					
M06		B3LYP		M06-2X	
EtCl	EtI	EtCl	EtI	EtCl	EtI
3.31	2.97	1.24	1.23	2.13	1.72

Comparing EtX Dissociation: Single Dimer vs. Across Double Dimer

The barriers for EtX dissociation on a single Si(100) dimer and across a double dimer were investigated at the B3LYP-D3/6-311+G(3df,p) level. The barriers can be found in Table S4. The single dimer EtX dissociation is 30.4 kJ/mol (EtCl) and 28.7 kJ/mol (EtI) than the barriers for dissociation across a double dimer.

Table S4. Barriers for EtX dissociation on single Si(100) and across a double Si(100) dimer. Barriers are given in kJ/mol.

Dissociation Energies (kJ/mol)		
	EtCl	EtI
Single Dimer	56.0	69.1
Double Dimer	86.4	97.8

Figure S1 shows the products of dissociation across the double dimer. Not only are the barriers to dissociation higher, but the double dimer dissociated products are less stable. Table S2 shows the dissociation energy for dissociation on the single dimer and dissociation across the double dimer.
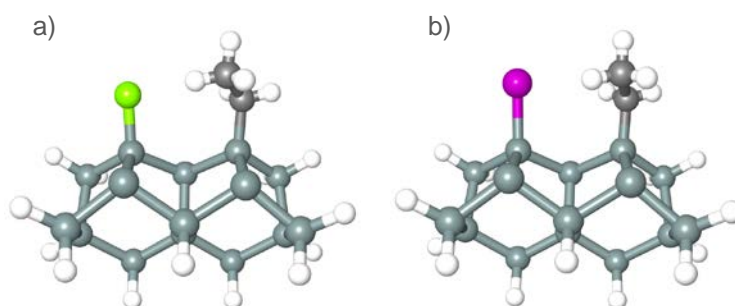

Figure S1. Geometries of a) EtCl and b) EtI dissociated across a double dimer cluster.

Table S5. Dissociation energies (in kJ/mol) for EtX dissociation on single Si(100) and across a double Si(100) dimer.

	EtCl	EtI
Single Dimer	−298.5	−275.3
Double Dimer	−259.3	−232.0

Reaction Profiles of All Functionals with and without Dispersion Corrections

Figure S1 summarizes how the addition of dispersion corrections affect the reaction profiles of B3LYP, M06, and M06-2X. The non-covalent interaction complex of the haloethane and the Si(100) dimer requires an accurate description of dispersion. M06 and M06-2X see changes from 2-6 kJ/mol with the addition of dispersion, while B3LYP complexation energies change by 20-28 kJ/mol. The M06 and M06-2X functionals already have some dispersion effects inherent in their parameterization.
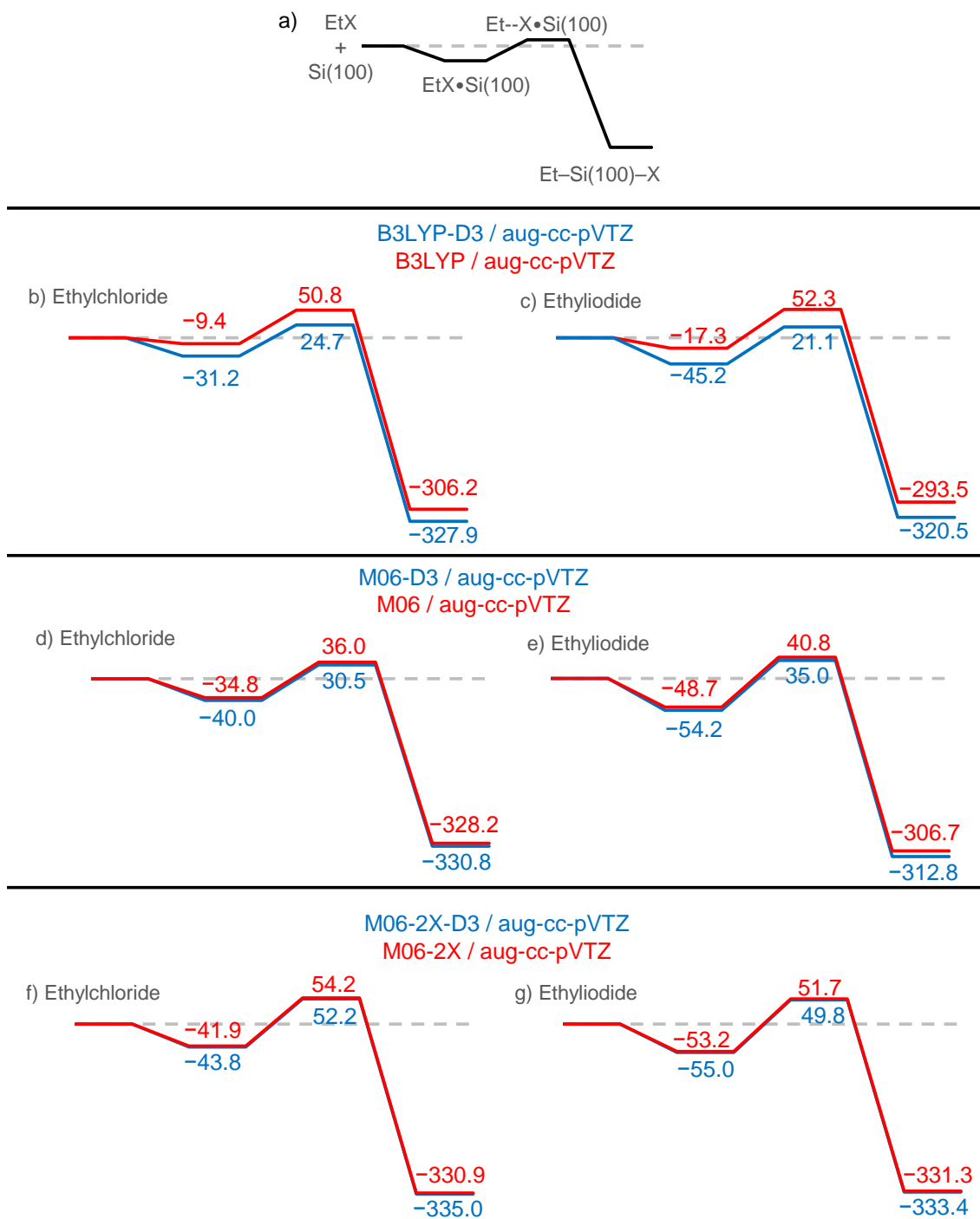
Figure S2. Summary of B3LYP, M06, and M06-2X zero-point corrected energy profiles with and without dispersion effects. Energies are in kJ/mol. Red lines indicate no dispersion corrections, blue lines indicate dispersion corrections are included. a) Scheme of the energy profiles of the haloethane non-covalently adsorbing, going through a transition state to dissociation, and the dissociated product. b) Ethylchloride B3LYP results. c) Ethyliodide B3LYP results. d) Ethylchloride M06 results. e) Ethyliodide M06 results. f) Ethylchloride M06-2X results. g) Ethyliodide M06-2X results.

Basis Set Effects on the Energetics of the Interaction Complex and Dissociation Activation Barrier

We have investigated how the formation of the interaction complex and the dissociation barrier changes with the cc-pVDZ, aug-cc-pVDZ, cc-pVTZ, aug-cc-pVTZ, and 6-311+G(3df,p) basis sets. The complexation energy of the intermediate is added to the activation barrier of ethyl halide dissociation to yield an effective barrier. Table S6 below summarizes these quantities calculated with the aforementioned basis sets and the M06-D3 functional. For the EtCl complexation energies, it varies only by 1.5 kJ/mol or less. EtI complexation energies change by 3.7 kJ/mol or less.

Comparing the effective dissociation barrier, all of the correlation consistent basis sets give effective barriers that are within 4.5 kJ/mol, suggesting that the effective barriers are roughly equal. The aug-cc-pVTZ basis set does yield a lower effective barrier compared to the other correlation consistent basis sets, but the small difference between the EtCl and EtI effective barriers persist. The 6-311+G(3df,p) basis set results in an effective EtCl dissociation barrier that is 8.2 kJ/mol lower than that of EtI. We attribute this difference between aug-cc-pVTZ and 6-311+G(3df,p) basis sets to the additional set of d and f functions present in the former basis set.

Table S6. Summary of basis set effects for the complexation energy of the intermediate, activation barrier for ethylhalide dissociation, and effective dissociation barrier for the M06-D3 functional and cc-pVDZ, aug-ccpVDZ, cc-pVTZ, and aug-cc-pVTZ basis sets. All energies are in kJ/mol.

	Complexation Energy (kJ/mol)		Dissociation Activation Barrier (kJ/mol)		Effective Dissociation Barrier (kJ/mol)	
Basis Set	EtCl	EtI	EtCl	EtI	EtCl	EtI
cc-pVDZ	-39.1	-50.5	86.2	94.7	47.0	44.2
aug-cc-pVDZ	-40.6	-52.4	83.9	95.9	43.3	43.5
cc-pVTZ	-40.3	-54.1	83.6	101.7	43.3	47.6
aug-cc-pVTZ	-40.0	-54.2	70.5	89.2	30.5	35.0
6-311+G(3df,p)	-39.6	-52.5	71.2	92.4	31.7	39.9

Bond Lengths for Non-Covalent Interaction Complex and Dissociation Transition State

Tables S7 and S8 summarize the important bond lengths for describing the non-covalent interaction complexes and transition states for ethylhalide dissociation on the Si(100) dimer cluster. Scheme S1 clarifies which bond lengths are specified in the table. For the ethyl halide dissociation transition state, the geometries are mostly dependent on the choice of functional, and B3LYP has a smaller dependence on the dispersion corrections compared to the changes observed in the non-covalent interaction complex. This is consistent with the relatively small change in absolute barrier height observed between B3LYP and B3LYP-D3. Comparing B3LYP-D3 and M06-D3, the Si–C bond length changes the most, with the M06-D3 distance shorter by approximately 0.15 Å. This suggests that M06-D3 gives a later transition state than B3LYP-D3, resulting in a higher barrier according to Hammond's postulate. The transition state C–X and Si–X bonds are relatively constant among all of the functionals, indicating the Si–C bond formation is the dominant internal coordinate to describe the dissociation. The geometries for M06 and M06-2X are not significantly affected by dispersion. The M06-2X-D3 bond lengths most differ for the Si–C bond in the dissociation transition states, which is consistent with the larger absolute barriers yielded by M06-2X-D3.
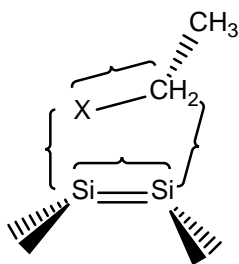
Scheme S1. Generic EtX interacting with the Si dimer to illustrate which bonds are described in Tables S7 and S8. The brackets indicate the bonds of interest. The same atom pairs are considered for the transition states.

Table S7. Summary of the bond lengths in the EtCl complexes and transition states for the B3LYP, B3LYP-D3, M06-D3, and M06-2X-D3 functionals.

	EtCl Geometry Bond Lengths (Å)							
	Complex				Transition State			
Bond	B3LYP	B3LYP-D3	M06-D3	M06-2X-D3	B3LYP	B3LYP-D3	M06-D3	M06-2X-D3
Si-Si	2.30378	2.31989	2.29206	2.31249	2.36175	2.36916	2.34244	2.34173
Si-C	3.86756	3.76894	3.6778	3.68263	3.63249	3.57635	3.41458	3.29823
Si-X	2.67887	2.54951	2.59707	2.46487	2.17588	2.16985	2.16451	2.14828
C-X	1.83548	1.84452	1.82185	1.82099	2.50411	2.4981	2.47107	2.54217

Table S8. Summary of the bond lengths in the EtI complexes and transition states for the B3LYP, B3LYP-D3, M06-D3, and M06-2X-D3 functionals. Bond lengths are listed in angstroms.

	EtI Geometry Bond Lengths (Å)							
	Complex				Transition State			
Bond	B3LYP	B3LYP-D3	M06-D3	M06-2X-D3	B3LYP	B3LYP-D3	M06-D3	M06-2X-D3
Si-Si	2.32701	2.33803	2.32067	2.32396	2.37872	2.38362	2.35393	2.35413
Si-C	3.83722	3.76224	3.65997	3.70507	3.52821	3.49677	3.34873	3.2392
Si-X	2.91303	2.83006	2.77493	2.77211	2.55754	2.54768	2.53427	2.52198
C-X	2.19756	2.20376	2.1601	2.16873	2.93619	2.95144	2.9288	2.90399

Iodine 6-311+G(3df,p) Basis Set Information
The following coefficients are formatted to be used in the Gaussian09 program.


```
I    0
S  5  1.00
 444750.0000000        0.0008900
  66127.0000000        0.0069400
  14815.0000000        0.0360900
   4144.9000000        0.1356800
   1361.2000000        0.3387800
S  2  1.00
    508.4400000        0.4365900
    209.5900000        0.1837500
S  1  1.00
     81.9590000        1.0000000
S  1  1.00
     36.8050000        1.0000000
S  1  1.00
     13.4950000        1.0000000
S  1  1.00
      6.8859000        1.0000000
S  1  1.00
      2.5520000        1.0000000
S  1  1.00
      1.2088000        1.0000000
S  1  1.00
      0.2734000        1.0000000
S  1  1.00
      0.1009000        1.0000000
SP  1  1.00
      0.0252250        1.0000000
P  4  1.00
```

```
   2953.6000000          0.0122100
    712.6100000          0.0858700
    236.7100000          0.2949300
     92.6310000          0.4784900
P  1  1.00
     39.7320000          1.0000000
P  1  1.00
     17.2730000          1.0000000
P  1  1.00
      7.9570000          1.0000000
P  1  1.00
      3.1529000          1.0000000
P  1  1.00
      1.3328000          1.0000000
P  1  1.00
      0.4947000          1.0000000
P  1  1.00
      0.2160000          1.0000000
P  1  1.00
      0.0829300          1.0000000
D  3  1.00
    261.9500000          0.0314400
     76.7340000          0.1902800
     27.5510000          0.4724700
D  1  1.00
     10.6060000          1.0000000
D  1  1.00
      3.4217000          1.0000000
D  1  1.00
      1.1370000          1.0000000
D  1  1.00
      0.9060000          1.0000000
D  1  1.00
      0.3020000          1.0000000
D  1  1.00
      0.1006667          1.0000000
F  1  1.00
      0.4064000          1.0000000
****
```